



ELSEVIER

Available online at www.sciencedirect.com

SCIENCE @ DIRECT®

Superlattices and Microstructures 38 (2005) 336–343

Superlattices
and Microstructures

www.elsevier.com/locate/superlattices

Defects in electron irradiated ZnO single crystals

M.A. Hernández-Fenollosa, L.C. Damonte, B. Mari^{*}

Department de Física Aplicada, Universitat Politècnica de València, Camí de Vera s/n, 46071-Valencia, Spain

Available online 15 September 2005

Abstract

Point defects were introduced in ZnO single crystals by means of irradiation with several fluences of 10 MeV electrons giving rise to irradiation doses between 60 and 240 Gy. Irradiation defects were subsequently studied by positron annihilation lifetime spectroscopy (PALS), a sensitive technique for investigating open volume defects and photoluminescence (PL). After irradiation, samples were annealed in an air atmosphere from 100 to 1000 °C in order to follow the evolution of irradiation defects and their effect on the emission properties. Positron lifetimes and intensities measured by PALS as a function of radiation doses show that the defects generated act as effective positron traps. The PL spectra for all the samples analysed consist of a near-band-edge (NBE) emission centred at 369 nm and a broad deep-level (DL) emission around 550 nm. The main observation is that the most intense PL emission is found for the higher electron dose used, i.e. 240 Gy. This effect is similar to that observed after processes leading to an improvement of the crystal quality, but it should be interpreted as arising from the annihilation of the non-radiative recombination centres, which strongly enhances the radiative recombination mechanisms. The trends observed using both experimental techniques were discussed in terms of the possible origin, nature and state of charge of the radiation induced defects involved.

© 2005 Elsevier Ltd. All rights reserved.

^{*} Corresponding address: Departament de Física Aplicada, ETS d'Enginyeria del Disseny, Universitat Politècnica de València, 46022 València, Spain. Tel.: + 34 963 877 525; fax: +34 9630 877 189.

E-mail addresses: mhernan@fis.upv.es (M.A. Hernández-Fenollosa), ldamont@upvnet.upv.es (L.C. Damonte), bmari@fis.upv.es (B. Mari).

1. Introduction

Zinc oxide (ZnO) is a promising material for many applications such as in pigments, piezoelectric transducers and optical devices. Recently, ZnO has attracted interest as a material for use in ultraviolet (UV) and blue light emitting devices because of its wide band gap of 3.37 eV and large exciton-binding energy of 60 meV. Taking advantage of these interesting properties, the realization of ZnO based optoelectronics devices seems to be very promising, but some requirements such as the realization of p–n junctions and good quality substrates are lacking.

Large-size ZnO single crystals grown by the hydrothermal method have been recently demonstrated [1] and are nowadays commercially available. Intrinsic and induced point defects in ZnO lead to the generation of bounded states having important effects on the material properties. A complete knowledge of point defect structure is then needed to improve the quality of ZnO substrates.

We have used two experimental techniques highly sensitive to defects: positron annihilation lifetime spectroscopy (PALS), well adapted for open volume defects studies [2], and photoluminescence (PL), to probe the changes in the optoelectronic properties of the crystals.

The PALS technique is based on the measurement of the positron lifetime inside the material studied. After the positron reaches thermal equilibrium with the host material it eventually annihilates an electron leading to the emission of gamma rays, which gives the experimental information. The annihilation can take place in interstitial regions characterized by an extended Bloch state (free state) or as trapped positrons in a bound state. Different kinds of defects (such as monovacancies, larger vacancy clusters, dislocations) can act as trapping centres, but only neutral or negatively charged ones can be effective positron traps [3].

Several contributions by means of positron annihilation methods have been made to the study of the nature of defects in Zn-related II–VI semiconductors powders and ceramics [4–8]. More recently, new defect studies on electron irradiated single crystals [9] and thin films on different substrates of ZnO samples [10] have also been published, using positron techniques. In some of them [5,7,8] the authors combined this technique with cathodoluminescence measurements and no correlation was found between the positron traps and luminescence centres.

In this work, we report the study of the point defects produced in hydrothermal ZnO single crystals by means of 10 MeV electron irradiation. The evolution of the irradiation defects, as seen using PALS and PL, was followed as a function of the annealing temperature.

2. Experimental procedure

ZnO (0001) single crystals were exposed to different 10 MeV electron fluences in successive steps of 60 Gy giving rise to irradiation doses up to 240 Gy. ZnO samples commercially available (Techno Chemicals, Japan) were grown by the hydrothermal method, which is known as a method for growing highly crystalline and large-size crystals at a relatively low temperature. After irradiation, the samples, having received a total dose of

Table 1
Positron annihilation parameters for different radiation doses

Dose	τ_1 (ps)	I_1 (%)	τ_2 (ps)	I_2 (%)	τ_{ave} (ps)
0	187 ₃	77 ₂	379 ₁₃	22 ₂	227
60	194 ₄	64 ₃	379 ₁₁	32 ₃	245
120	192 ₃	72 ₂	385 ₁₁	26 ₂	238
180	191 ₃	77 ₂	395 ₁₂	21 ₂	230
240	193 ₄	73 ₃	388 ₁₇	24 ₃	234

τ_i , I_i are the lifetime and corresponding intensity for state i .

τ_{ave} is the average lifetime: $\tau_{\text{ave}} = \sum I_i \tau_i$.

120 and 240 Gy, were annealed in an air atmosphere for 10 min, at different temperatures from 100 to 1000 °C in steps of 100 degrees, and then quenched to room temperature (RT).

PALS measurements were collected at room temperature in a conventional fast–fast coincidence system with two scintillator detectors. The time resolution (FWHM) was 260 ps and 3×10^6 counts were accumulated for each spectrum. The radioactive source, $^{22}\text{NaCl}$ (10 μCi), was deposited onto a Kapton foil (1.42 g/cm³) and sandwiched between two sample specimens. The source contribution (17% of 386 ps for the annihilation in Kapton foil and 1% of 2.0 ns) and the response function were evaluated using a reference sample (Ni metal), using the RESOLUTION code [11].

The PL study was performed using the 325 nm emission line of a He–Cd laser. The sample was moved under a stationary laser spot using an x – y – z stage on which a closed cycle helium cryostat was mounted. The beam was focused down to a spot of diameter ~ 200 μm on the sample, which was held at several temperatures in the range from 20 K to RT, in order to record the PL signal at different temperatures. Spectra were recorded using a grating monochromator coupled to a back-thinned CCD cooled by the Peltier effect.

3. Results and discussion

The lifetime spectra for the as-grown and irradiated samples were decomposed into three exponential decays, $n(t) = \sum_i I_i \exp(-t/\tau_i)$, each being positron state characterized by a positron lifetime, τ_i , with a certain intensity, I_i ($\sum_i I_i = 1$). This positron state can be a delocalized state in the lattice (the bulk lifetime) or a localized state at a defect site. Table 1 shows the positron lifetime parameters obtained for irradiated samples at different radiation doses. The long lifetime component ($1.6 < \tau_3 < 1.9$ ns with intensity around 1.5–2.5%) for all cases is due to annihilation in the source itself (not shown in Table 1).

The minor lifetime, τ_i , obtained for the non-irradiated sample agrees with previous reported values of the bulk lifetime in ZnO material [4,7,9].

One useful parameter, almost independent of the data treatment, is the average positron lifetime defined by $\tau_{\text{av}} = \sum_i I_i \tau_i$. From this statistical parameter, one can extract information about positron trapping when a separation into different components with similar positron lifetime is not possible. The calculated average lifetime for irradiated samples is also shown in the last column of Table 1. We can observe that τ_{av} increases with the first irradiation step, diminishes with the following two doses and increases again

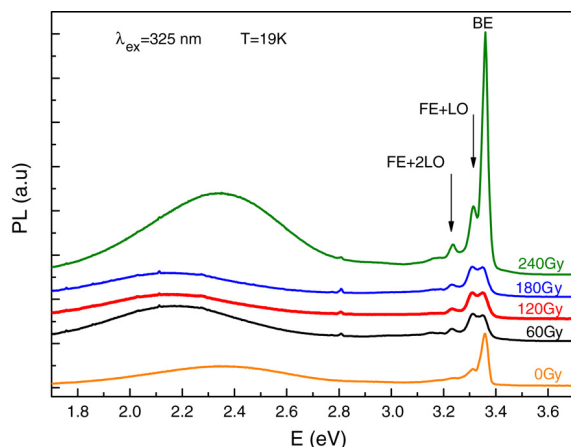


Fig. 1. PL spectra of the electron irradiated samples as recorded at 19 K.

with the 240 Gy dose. The variation of average lifetime with dose indicates that positrons are annihilated in different positron states. In a previous work [12] we have discussed this behaviour together with photoluminescence results, taking into account the charge state of the involved defects.

Fig. 1 shows the photoluminescence spectra at 19 K for the irradiated samples. The luminescence spectra for all the samples analysed consist of the near-band-edge (NBE) emission (centred at 3.36 eV) and the deep-level (DL) emission (in the 2.2–2.4 eV region). In the excitonic part of the PL spectra three narrow peaks corresponding to the bound exciton (BE) and two phonon replicas appear. The bound exciton peak reduces its intensity with the irradiation. This value remains constant up to the highest fluence (240 Gy) where a sudden increase of its intensity, reaching even higher values than for non-irradiated material, is observed. The enhancement of the excitonic part of the PL spectrum is usually assigned to an improvement of the crystal quality [13], which is not appropriate here since point defects have been introduced by high energy electron irradiation. Therefore this effect should be due to an exhaustion of the non-radiative recombination mechanisms which are always in competition with the radiative ones [12]. The exhaustion of the non-radiative route is related to the reorganization of the different kinds of defects as a consequence of the amount of new radiation induced defects present.

The intensity of the DL band emission exhibits a similar behaviour, but additionally its energy centre shows a shift towards lower energies. A huge variety of defects (oxygen vacancies (V_O), zinc vacancies (V_{Zn}), interstitial zinc (Zn_i), interstitial oxygen (O_i) and antisite oxygen (O_{Zn})) have been suggested to contribute to the broad green band in ZnO [14–16]. Taking into account this population of possible defects, we think that the DL band shift is due to the different natures of defects present in the sample for the various irradiation doses.

As is shown in the Fig. 1, the DL band is localized around 2.38 eV for the as-grown and 240 Gy samples, but for the rest of the irradiation doses the position goes to lower energies (~ 2.2 eV). Since the observed trends in the DL band seem different for different radiation

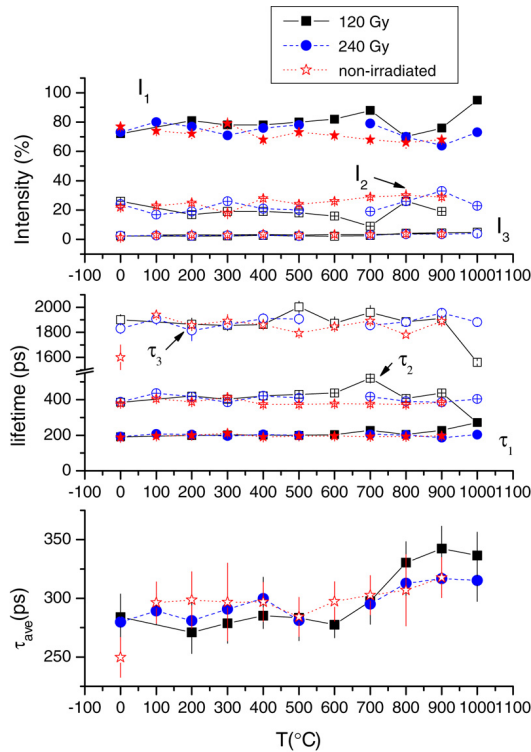


Fig. 2. Positron lifetime parameters versus annealing temperature. Star (\star): non-irradiated; square (\blacksquare): 120 Gy dose; circle (\bullet): 240 Gy dose samples.

doses, the 120 Gy (sample A) and 240 Gy (sample B) irradiated samples were heat treated at different temperatures with the aim of identifying the radiation defects.

Fig. 2 shows the evolution of the positron lifetime parameters with annealing temperature of both irradiated samples together with a non-irradiated one for comparison. The fitting procedure, without constraints, also yields three lifetime components. The lower one is mainly associated with annihilation in the bulk of the material. The second one can be considered as a mean value of two processes: the annihilation of positrons in attractive defects (localized states) together with the principal source (Kapton) contribution. Meanwhile the longer lifetime is due to annihilation in the source itself. For sample B at the first annealing step these values result: $\tau_1 = 207_2$ ps, $I_1 = 80_1\%$, $\tau_2 = 436_{14}$ ps, $I_2 = 17_1\%$, $\tau_3 = 1.91_5$ ns, $I_3 = 2_1\%$. Similar values are obtained for sample A. It can be observed that the annihilation parameters in this first step are rather different to the corresponding ones for the as-irradiated sample before annealing. In particular, the two main positron lifetimes are higher. This leads to fluctuations in the average positron lifetime that persisted up to an annealing temperature of 600 °C. This behaviour may be attributed to some reorganization of defects at these low temperatures.

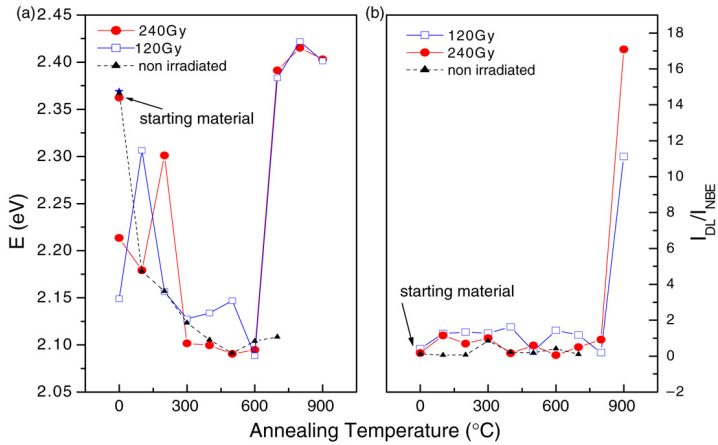


Fig. 3. Analysis of the PL data. The graphs show the energy position for the DL emission band and the ratio between the DL and NBE bands versus the annealing temperature.

Experimental and calculated values for the positron lifetime in ZnO free of defects of 183₄ ps and 177 ps, respectively, were reported [7,9]. After sintering ZnO ceramics at 1200 °C, a second positron lifetime of 255₁₆ ps was obtained, ascribed to cation vacancies [8]; meanwhile the Zn vacancy calculated value results as 237 ps [9]. So we can conclude that in our case, both τ_1 and τ_2 take into account some kinds of defects.

After the 600 °C annealing, the average positron lifetime suddenly increases, indicating the presence of new attractive positron traps. A noticeable feature in this range of temperatures is that the intensity of the long component increases progressively, from 2% up to 5% after 1000 °C. Moreover, in this last stage, the positron spectrum for sample A can be well fitted with two components, their values being 272₁ ps and 1.60₁ ns and their respective intensities 95₁ and 5.0₁.

For the two lifetimes $\tau_{D1} = 211_2$ ps (sample A first annealing step) and $\tau_{D2} = 272_1$ ps (sample A last annealing step), we can evaluate the ratio τ_D/τ_b , which is related to the defect size. The result yields the values 1.1 and 1.49, respectively, where $\tau_b = 183$ ps was used [9]. So we can assign the defect D1 as a monovacancy and the D2 as a larger open volume defect such as a divacancy [3,7].

For the non-irradiated sample, one observes an increase in the average lifetime with the 100 °C annealing leading the value towards the as-irradiated sample one. Further treatments do not modify the lifetime parameters, at least up to 600 °C annealing. Therefore, we can conclude that the annealing at 100 °C for the non-irradiated sample has the same effect as electron irradiation on ZnO single crystals.

The PL spectra for the three annealed samples were also taken at 19 K and displayed the characteristic two bands. The analysis of these spectra is shown in Fig. 3. Fig. 3(a) shows the positions in energy of the DL emission and three main facts become very clear: (a) just the irradiation in the annealing to 100 °C of the starting material produces a shift from 2.37 eV to lower energies; (b) a continuous decrease in energies until the annealing at 600 °C occurs is followed for the three samples analysed, except for two singular points

at 100 °C for the 120 Gy and 200 °C for the 240 Gy cases; (c) there is a drastic change to higher energies for higher annealing temperatures in the case of the irradiated samples. The PL intensity ratio of the DL emission to the NBE emission versus annealing temperature is shown in Fig. 3(b); this ratio shows a big change only for the irradiated samples from 800 °C.

We can approach an assignment of the centres responsible for the observed evolution with annealing temperature for both the average positron lifetime and the PL parameters. As discussed above, the two techniques display similar behaviours during the annealing steps. We propose the following explanation. At the first stage of annealing and after electron irradiation, monovacancies are induced. As these are seen by PAS, the negatively charged ones are the candidates, i.e. V_{Zn} . With progressive annealing, reorganization of defects takes place up to 600 °C, yielding the fluctuations observed in the DL band position. Above 600 °C annealing, new attractive centres are generated, identified by means of positrons as divacancies or clusters, due to the higher positron lifetime.

4. Conclusion

Two different methods have been applied in order to study point defects in ZnO substrates. It has been shown that accumulative radiation doses have a similar effect to that observed after processes leading to an improvement of the crystal quality, but this should be interpreted as arising from an annihilation of the non-radiative recombination centres, which strongly enhances the radiative recombination mechanisms.

Parameters of both techniques showing the same behaviours with annealing temperature have been identified, allowing us to infer possible natures of the defects. In order to unequivocally identify the radiation and thermally induced defects involved, measurements at different temperatures are now in progress.

Acknowledgement

This work was supported by the MCYT (Spain) under grant MAT2002-04539-C02-02.

References

- [1] T. Sekiguchi, S. Miyashita, K. Obara, T. Shishido, N. Sakagami, *J. Cryst. Growth* 214–215 (2000) 72.
- [2] P. Hautojarvi (Ed.), *Positrons in Solids*, Springer-Verlag, Berlín, 1979;
W. Brandt, A. Dupasquier (Eds.), *Positron Solid State Physics*, North-Holland Pub. Co., Amsterdam, 1983.
- [3] M.J. Puska, R.M. Nieminen, *Rev. Modern Phys.* 66 (1994) 841.
- [4] R.M. de la Cruz, R. Pareja, R. González, L.A. Boatner, Y. Chen, *Phys. Rev. B* 45 (1992) 6581.
- [5] W. Puff, S. Brunner, P. Mascher, G. Balogh, *Mater. Sci. Forum* 196–201 (1995) 333–338.
- [6] S. Brunner, W. Puff, P. Mascher, G. Balogh, H. Baumann, *Mater. Sci. Forum* 258–263 (1997) 1419–1424.
- [7] R. Krause-Rehberg, H.S. Leipner, T. Abgarjan, A. Polity, *Appl. Phys. A: Mater. Sci. Process.* 66 (1998) 599–614.
- [8] J. Zhong, P. Mascher, W. Puff, A.H. Kitai, *Mater. Sci. Forum* 143–147 (1994) 465.
- [9] F. Tuomisto, V. Ranki, K. Saarinen, D.C. Look, *Phys. Rev. Lett.* 91 (2003) 205502.
- [10] A. Uedono, T. Koida, A. Tsukazaki, M. Kawasaki, Z.Q. Chen, S.F. Chichibu, H. Koinuma, *J. Appl. Phys.* 93 (2003) 2481–2485.

- [11] P. Kirkegaard, M. Eldrup, *Comput. Phys. Commun.* 3 (1972) 240; 7 (1974) 401.
- [12] L.C. Damonte, M.A. Hernández-Fenollosa, B. Marí, *Appl. Phys. Lett.* (2005) (submitted for publication).
- [13] J.A. Sans, A. Segura, M. Mollar, B. Marí, *Thin Solid Films* 453–454 (2004) 251.
- [14] F. Leiter, H. Alves, D. Pfisterer, N.G. Romano, D.M. Hofmann, B.K. Meyer, *Physica B* 340–342 (2003) 201.
- [15] J. Lim, K. Shin, H.W. Kim, C. Lee, *Mater. Sci. Eng. B* 107 (2004) 301.
- [16] J. Wang, G. Du, Y. Zhang, B. Zhao, X. Yang, D. Liu, *J. Cryst. Growth* 263 (2004) 269.